

Parametric failure limit detection for the sheet metal forming of a floating photovoltaic (FPV) aluminum alloy structure

TVEIT Sigbjørn^{1,a*}, REYES Aase^{1,b} and ERDURAN Emrah^{1,c}

¹Department of Built Environment, Oslo Metropolitan University, Postboks 4, St. Olavs plass, NO-0130 Oslo, Norway

^asigbjorn.tveit@oslomet.no, ^baase.reyes@oslomet.no, ^cemrah.erduran@oslomet.no

Keywords: Sheet Metal Forming, Aluminum Alloys, Parametric Analysis

Abstract. The sheet metal forming process of a floating photovoltaic (FPV) structure is simulated in LS-DYNA. An anisotropic yield criterion and a two-term Voce hardening law are used to model the plastic behavior of AA5083-H111 sheets. The numerical model incorporates thickness variations to trigger local necking and uses a critical thickness strain as a fracture criterion. To establish a methodology that can be expanded for further studies, the research explores the relationship between cup depth and drawbead distance by proposing an algorithm to distinguish between successful and unsuccessful sheet metal forming operations.

Introduction

In the competitive race of developing new methods for renewable energy production, the floating solar producer Sunlit Sea AS has come up with an innovative solution where formed aluminum alloy sheet structures are used as supports for floating photovoltaic (FPV) panels. In each FPV float, two formed components are joined together back-to-back, and sealed off along the rim to create a buoyant platform. The choice of material represents a key attribute of the design: As the power output of FPV modules decreases at elevated operational temperatures, the highly conductive aluminum alloy body, which acts as a thermal bridge between the FPV module and the cool sea water, allows the units to operate with increased efficiency.

A critical feature in the design is the repeated cup shape, which acts as a spacer to provide structural integrity to the platform. This allows for walking on top of the solar panels, which facilitates effortless installation, operation, and maintenance. The cup depth directly influences the buoyancy of the platform, and, as the cups transfer heat and forces, their geometry and constellation have a massive influence on the FPV's operational performance. Hence, for the technology to reach its potential with respect to cost per unit energy output, the optimization of the structural geometry with respect to several parameters, including the heat transfer, and the material costs, is vital.

A challenge emerges in the radical deep-drawing of marine-grade aluminum, as aggressively pushing the drawing limit can lead to increased failure rates in the production line. Sunlit Sea's collaborative partners have painstakingly developed a shape that is feasible to manufacture by deep-drawing 1.5 mm thick AA5083-H111 sheets close to their forming limit. However, in developing the next generation of floats, the company seeks a more flexible and efficient design process, that enables rapid testing of multiple design variations in a virtual environment, by combining explicit non-linear finite element (FE) simulations in LS-DYNA [1], with machine learning techniques.

As an initial part of this work, the current paper presents the precursory investigations of the comprehensive study on the influence of various geometric parameters on the sheet metal forming process of the Sunlit Sea's FPV structure. The overarching aim of the ongoing study is to establish a parametrized FE model that can be used to generate data for the training of an artificial neural network (ANN) that will be applied in the optimization process to develop the structural design

for the FVP system. While the investigation presented in this paper is limited, its findings will be used as a basis to develop the methodology for the further research.

In the realm of machine learning classification, decision boundaries are used to distinguish classes. In order to efficiently train the ANN to classify whether a sheet metal forming process will be successful or not for a given set of process parameters, it is crucial to assure the quality of the training data. Ideally, the database should be balanced, with roughly the same number of instances in the different classes, i.e. successful and unsuccessful forming operations [2]. Consequently, it is advantageous to get a sense of the mutual dependencies between important process parameters when generating the training data. Moreover, the predictive capability of the trained model relies on the accuracy of the training data, which calls for precise numerical models equipped with capable phenomenological models that accurately capture the material behavior.

As sheet metals are plastically deformed into complex shapes, a series of plastic instabilities may occur, as the material is subjected to large strains. The sequence of instability phenomena is normally initiated by diffuse necking, followed by localized necking and/or shear instability, until the coalescence of voids concludes in ductile failure [3]. While diffuse necking is often regarded as acceptable in industrial practices, the onset of a localized neck, or a shear localization, is commonly referred to as the material's forming limit.

Over the years, considerable research has been dedicated to the development of phenomenological models aiming to describe the occurrence of the various plastic instabilities that govern formability. Marciniak and Kuczynski (MK) [4] described how the presence of an imperfection, such as a small reduction in thickness, or an inhomogeneity in the material characteristics, causes the plastic strains to localize for sheet metals in biaxial tension. Since then, the concept has been further developed [5], and employed in conjunction with advanced anisotropic plasticity models, demonstrating the significance of the yield function and the plastic strain hardening law on the predicted forming limits. The MK approach has also been implemented in non-linear FE codes, where a non-local instability criterion (NLIC) is used to detect strain localization that are triggered by imperfections in the form of randomly distributed thickness variations [6-8]. A through-thickness shear instability criterion (TTSIC) was proposed by Bressan and Williams [9] for applications in isotropic sheet metals, a formulation that was later generalized by Hopperstad et al. [10] to comply with materials with orthotropic anisotropy. Reyes et al. [11] proved the robustness of NLIC and TTSIC when used in an FE model with random shell thickness variations, by demonstrating that the models could predict the decreased formability observed for certain aluminum alloy sheet metals subjected to biaxial pre-strain.

In this work, the deep-drawing of the indented cups in Sunlit Sea's FPV structure is simulated using a non-linear finite element model in LS-DYNA. A non-quadratic anisotropic yield criterion [12] with the associated flow rule, and a two-term Voce hardening law [13] are used to describe the plastic behavior of the sheet metal. Microscopic sheet thickness variations are implemented to trigger localized necking, and a simple fracture criterion based on a critical thickness strain is employed [14]. To establish a methodology that can be expanded upon in further studies, the model is used to explore the relationship between two geometric parameters: cup depth and drawbead distance. A simple algorithm is proposed to determine the curve that separates successful and unsuccessful sheet metal forming operations in the two-dimensional parameter space.

Material models

The anisotropic Yld2003 [12], referred to in the LS-DYNA keyword as the strong texture model (STM), was employed as yield criterion, and as plastic potential by adopting the associated flow rule. The function is a generalization of the isotropic Hershey-Hosford yield function, which, for plane stress, can be written as

$$|\sigma_1|^m + |\sigma_2|^m + |\sigma_1 - \sigma_2|^m = 2\sigma_Y^m \quad (1)$$

where σ_Y is the flow stress. σ_1 and σ_2 are the non-zero principal stress tensor components:

$$\left. \begin{matrix} \sigma_1 \\ \sigma_2 \end{matrix} \right\} = \frac{\sigma_x + \sigma_y}{2} \pm \sqrt{\left(\frac{\sigma_x - \sigma_y}{2}\right)^2 + \tau_{xy}^2} \quad (2)$$

The Yld2003 yield function introduces anisotropy by dividing the function in Eq. (1) into two separate parts:

$$\phi = \phi' + \phi'' = 2\sigma_Y^m \quad (3)$$

where

$$\phi' = |\sigma'_1|^m + |\sigma'_2|^m \quad (4)$$

$$\phi'' = |\sigma''_1 - \sigma''_2|^m \quad (5)$$

The generalized principal stress terms σ'_1 , σ'_2 , σ''_1 , and σ''_2 , are constructed analogous to the principal stress formulae in Eq. (2) as

$$\left. \begin{matrix} \sigma'_1 \\ \sigma'_2 \end{matrix} \right\} = \frac{a_8 \cdot \sigma_x + a_1 \cdot \sigma_y}{2} \pm \sqrt{\left(\frac{a_2 \cdot \sigma_x - a_3 \cdot \sigma_y}{2}\right)^2 + a_4^2 \cdot \tau_{xy}^2} \quad (6)$$

$$\left. \begin{matrix} \sigma''_1 \\ \sigma''_2 \end{matrix} \right\} = \frac{\sigma_x + \sigma_y}{2} \pm \sqrt{\left(\frac{a_5 \cdot \sigma_x - a_6 \cdot \sigma_y}{2}\right)^2 + a_7^2 \cdot \tau_{xy}^2} \quad (7)$$

Here, a_1 to a_8 are the eight anisotropy coefficients that can be calibrated to experimental flow stress ratios and strain ratios obtained in different directions of uniaxial tensile stress, as well as in equibiaxial tensile stress, or a stress state that is equivalent with respect to the deviatoric stress.

For uniaxial tension at an angle θ to the sheet's rolling direction (RD), the strain ratio is defined as

$$R_\theta = \frac{d\varepsilon_w}{d\varepsilon_t} \quad (8)$$

where $d\varepsilon_w$ and $d\varepsilon_t$ are respectively the incremental strains in the width and thickness direction of the specimen. Moreover, the uniaxial flow stress ratio is defined as

$$r_\theta = \left. \frac{\sigma_\theta}{\sigma_{\theta=0}} \right|_{W_p} \quad (9)$$

where σ_θ is the directional flow stress at a certain level of plastic work W_p .

The disc compression test generates a deviatoric stress state that is equivalent to that of equibiaxial tensile stress ($\sigma_b = \sigma_1 = \sigma_2$). As the plastic process is independent of the hydrostatic pressure, this simple test is used to experimentally measure the in-plane plastic strains of the

equibiaxial stress state [15]. By measuring the in-plane strains at different levels of compression, the incremental strains in TD and RD are obtained. The strain ratio in equibiaxial tensile stress is then taken as

$$R_b = \frac{d\varepsilon_{TD}}{d\varepsilon_{RD}} \quad (10)$$

where $d\varepsilon_{TD}$ and $d\varepsilon_{RD}$ are the incremental strains in the transverse and the rolling directions, respectively. Moreover, the equibiaxial stress ratio is typically obtained by comparing the yield stress measured in bulge tests, to that measured in a uniaxial tensile test in RD ($\theta = 0$):

$$r_b = \frac{\sigma_b}{\sigma_0} \quad (11)$$

Plastic strain hardening is modeled using the two-term Voce hardening rule [13], which reads

$$\sigma_Y(\varepsilon_{pl}) = \sigma_0 + \sum_{i=1}^2 Q_{Ri} [1 - \exp(-C_{Ri}\varepsilon_{pl})] \quad (12)$$

Here, ε_{pl} is the effective plastic strain, σ_0 is the stress at the onset of yielding, and Q_{Ri} and C_{Ri} are the Voce coefficients.

To trigger necking instability, which is quickly followed by failure, the material inhomogeneities were modeled as a field of random thickness variation, generated by spectral decomposition using Karhunen-Loève expansions [1, 16]. For this purpose, an isotropic Gaussian correlation function B was adopted:

$$B(t) = e^{-(at)^2} \quad (13)$$

where a is the correlation parameter. In LS-DYNA, the user has the option to use a random seed, which generates a new Gaussian random thickness field for every run, or to provide a fixed seed number, to facilitate a deterministic analysis. A scale factor f_{SCL} is employed to control the magnitude of the thickness perturbations.

A fracture criterion based on the local critical thickness strain was adopted [14]:

$$\varepsilon_t \leq \varepsilon_{t,cr} \quad (14)$$

where $\varepsilon_{t,cr}$ is the critical thickness strain as fracture.

Numerical model

Sunlit Sea's current design features 34 cups with center-to-center distance of 260 mm (see Fig. 1 (a)). The cups have a radius $r_{cup} = 80$ mm, and a depth $d_{cup} = 38.5$ mm. To avoid wrinkling in the drawing process, a circular drawbead is located at a distance $d_{db} = 5$ mm from the edge of the cup. A schematic diagram of the drawing operation of the cup is provided in Fig. 1 (b).

An FE model was established to simulate the sheet metal forming of the float component's cups in LS-DYNA R12.0. For simplicity, it was conservatively assumed that the drawbead, which circumferences the cup geometry, completely restricts any material flow. This assumption, which is conservative from a formability perspective, allows the sheet metal inside the drawbead to be modeled as a circular plate with a fixed constraint along its rim.

To allow the investigation of failure modes without restricting possible non-symmetric outcomes, the full circular symmetric cup system was modelled. The die and punch were modeled with rigid shell elements, based on the CAD geometry of the original forming press tool. The motion of the punch was prescribed according to a quadratic polynomial function, and the contact between the forming tools and the blank was modeled using a one-way surface-to surface rule, with a constant friction coefficient μ . Selective mass scaling was employed to reduce computational costs by accelerating the explicit time-integration scheme without introducing significant dynamic effects upon impact between the forming tools and the blank.

The deformable blank was modeled using reduced integration Belytschko-Tsay elements with five through-thickness integration points, and approximate lengths of 1.2 mm. The part was equipped with the material models described in the previous section, through the keyword *MAT_WTM_STM. The material parameters used in the input are reported in Table 1.

The parameters of the two-term Voce plastic strain hardening law were calibrated to stress-strain data from five parallel uniaxial tensile tests in RD [17], by minimizing an error function based on the sum of squared residuals.

The anisotropy coefficients of Yld2003 were calibrated in LS-DYNA to experimental data from [17]. Data from uniaxial tensile tests at $\theta = 0^\circ, 45^\circ,$ and 90° to RD provided the stress ratios r_θ , and the strain ratios R_θ . Moreover, the equibiaxial strain ratio R_b was obtained from the disc compression test data. Due to lack of experimental bulge test data, the equibiaxial stress ratio was assumed to be isotropic, $r_\theta = 1$. As is common practice for face-centered cubic (FCC) materials, the yield function exponent was taken as $m = 8$. In Fig. 2, the yield function's consistency with measurements from uniaxial tensile tests at seven different angles θ is demonstrated.

Through the *PERTURBATION keyword, the random distribution was modelled, creating microscopic deviations in the shell thickness among the elements in the blank. Due to the absence of specific data on the surface topology of the sheet metal used in the current study, the correlation parameter a was taken as unity, based on a qualitative assessment of the resulting thickness fields, while the perturbation scale factor was taken as $f_{SCL} = 0.005$ mm.

Experimental tests performed by Sunlit Sea's collaborative partners in the development of the design reportedly revealed that a cup depth of 40 mm resulted in failure, while a cup depth of 38.5 mm remained intact during forming, without showing any signs of neck formation. These reported results were used to estimate the constant friction coefficient μ , and the critical thickness strain at fracture $\epsilon_{t,cr}$, in the absence of detailed experimental evidence. To do this, the forming of the original geometry ($d_{cup} = 38.5$ mm), and a model with $d_{cup} = 40$ mm, were simulated using different friction coefficients, and the original drawbead distance $d_{db} = 5$ mm. To alter the cup

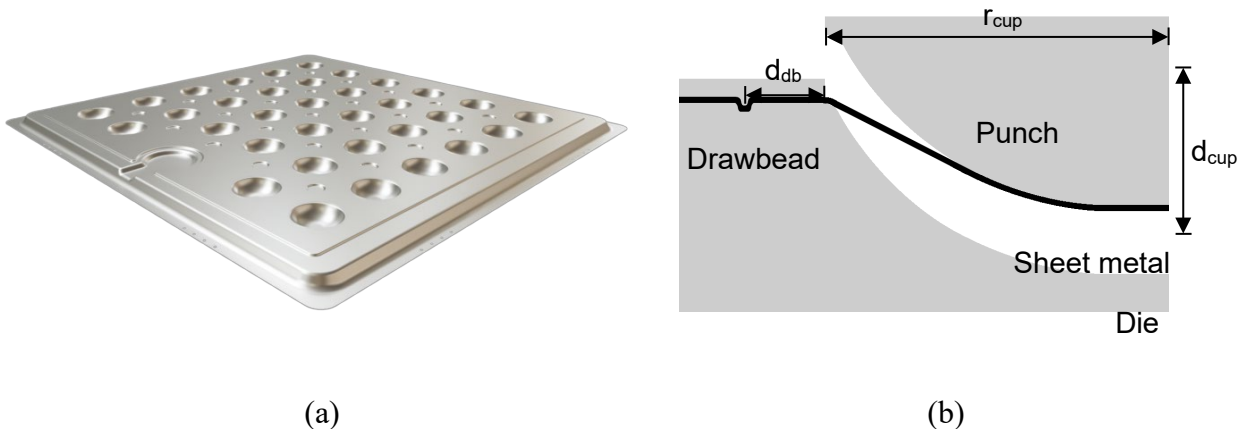


Fig. 1 (a) FPV structural component with repeated cup geometry, approximately 2 by 2 m in size; (b) sheet metal forming scheme of the indented cups of the FPV structure.

depth while keeping the initial tool distances of the native model, the vertical nodal coordinates of the drawing tools were scaled and shifted. Distributions of strains in the space of ϵ_1 and ϵ_2 were manually evaluated in order to determine a friction coefficient that did not predict necking at $d_{cup} = 38.5$ mm, while predicting significant necking at $d_{cup} = 40$ mm. Fig. 3 (a) and (b) respectively display the element strains in the entire cup for $d_{cup} = 38.5$ and 40.0 mm, with $\mu = 0.085$. It is apparent from the plot for $d_{cup} = 38.5$ mm that the strains in different elements are densely grouped in the strain space, while the plot for $d_{cup} = 40$ mm shows derivative strain levels in selected elements, indicating local neck formation. To comply with the reported observations, a critical thickness strain $\epsilon_{t,cr} = -0.45$ was adopted as a fracture limit. The sensitivity of $\epsilon_{t,cr}$ was analyzed, and it was concluded that the magnitude of $\epsilon_{t,cr}$ has insignificant impact on the predicted forming limits as long as plastic instability occurs before the thickness strain exceeds $\epsilon_{t,cr}$.

Detection of parametric failure limits

To establish a methodology that can later be expanded to a multidimensional parameter space, an algorithmic approach was developed to locate the curve that separates safe from unsafe configurations of process parameters. In the current study, the relationship between the drawbead distance d_{ab} , and the cup depth d_{cup} , was investigated (cf. Fig. 1 (b)). MATLAB scripts were developed to parametrize the model, by manipulating the LS-DYNA input files. As described in the previous section, the cup depth was controlled by scaling and shifting the nodal coordinates of the forming tool parts. To vary the drawbead distance, the radius of the circular blank was scaled, while the element size (approximately 1.2 mm) was kept as consistent as possible.

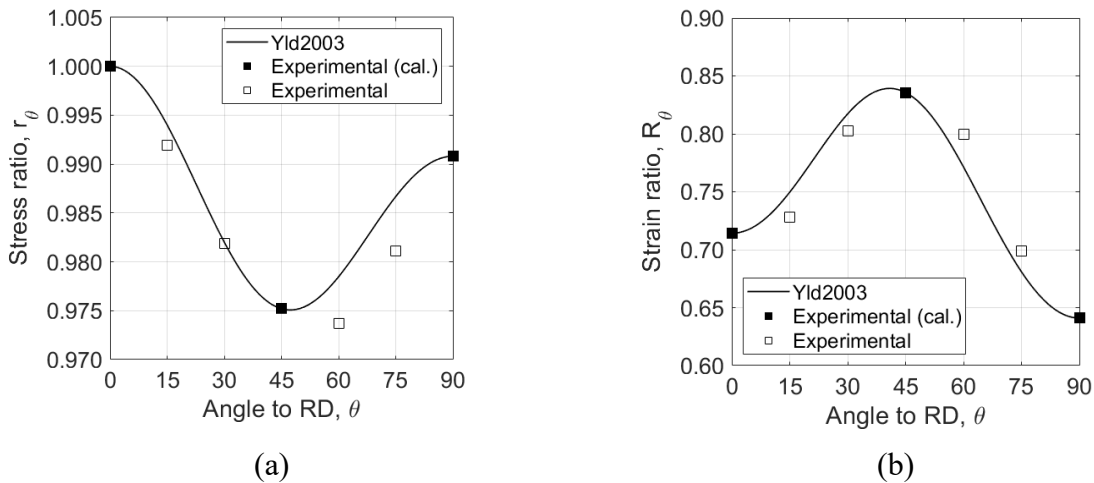


Fig. 2 (a) Stress- and (b) strain ratios vs. load angle for the fitted Yld2003 yield criterion and uniaxial test data from [17]. The solid markers represent the input for the calibration in LS-DYNA.

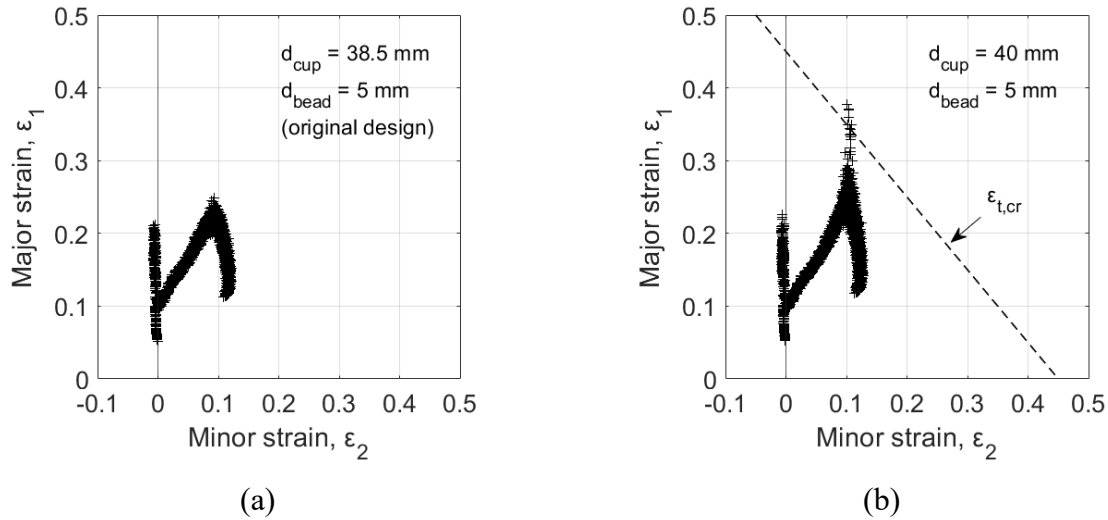


Fig. 3 Major and minor true strains from LS-DYNA used to estimate the friction parameter μ , and the critical thickness strain $\epsilon_{t,cr}$: (a) Original design ($d_{cup} = 38.5$ mm), and (b) with increased cup depth ($d_{cup} = 40$ mm).

Table 1 Model parameters

Elastic/mechanical properties								
Density, ρ [g/cm ³]			Young's modulus, E [N/mm ²]			Poisson ratio, ν [-]		
2.650			72000			0.33		
Yld2003 input [17]								
r_0 [-]	r_{45} [-]	r_{90} [-]	r_b [-]	R_0 [-]	R_{45} [-]	R_{90} [-]	R_b [-]	m [-]
1.000	0.9752	0.9908	1.000	0.7142	0.8357	0.6410	1.1263	8
Voce parameters								
σ_0 [MPa]		Q_{R1} [MPa]	C_{R1} [-]		Q_{R2} [MPa]	C_{R2} [-]		
153.7		94.33	2.352		187.1	15.35		
Perturbation parameters			Friction		Fracture			
a [-]	f_{SCL} [mm]		μ [-]		$\epsilon_{t,cr}$ [-]			
1.0	0.005		0.085		-0.45			

To search for the failure front in the two-dimensional parameter space, the following algorithm was developed. The drawbead distance d_{db} was taken as an independent variable, and a step size $\Delta d_{db} = 5$ mm was used to cover the parameter interval from $d_{db,min} = 5$ mm, the original geometry, to $d_{db,max} = 45$ mm, the maximum drawbead distance that can fit between the cups in the original constellation.

Since the model was calibrated to experience failure at a cup depth of 40 mm for a drawbead distance of 5 mm, the initial value $d_{cup,0}$ was taken as 39.5 mm at this drawbead distance, which predicts a successful forming operation, where the fracture criterion in Eq. (14) is not satisfied. With a step size of $\Delta d_{cup} = 0.5$ mm, the cup size was increased, and a new simulation was run with the updated variables. Upon the occurrence of a failed forming operation, d_{cup} was decreased

by half a step size in the next run, refining the prediction of the failure limit to a precision of $0.5 \cdot \Delta d_{cup}$. The algorithm then proceeded by increasing the drawbead distance by Δd_{db} , adopting the largest d_{cup} value that resulted in a successful forming operation, repeating the procedure, until d_{db} exceeds $d_{db,max}$. A flowchart of the search algorithm is provided in Fig. 4.

The results from the sensitivity analysis are displayed in Fig. 5. In Fig. 5 (a), the path taken by the algorithm is indicated with the dotted line connecting the datapoints, which represent the 32 different simulations that were run to complete the algorithmic search. The squares and crosses, respectively indicating the successful and unsuccessful forming processes, are separated by a solid line indicating the predicted parametric failure limit. It is evident from the plot that the FE model predicts a proportional relationship between the two parameters on the interval from $d_{db} = 5$ mm to 25 mm, after which a plateau is reached. When reviewing the presented results, it should be noted that the solid line in Fig. 5 (a) represents the predicted fracture, using the simple critical thickness strain criterion in Eq. (14), while the forming limit of sheet metals is typically taken as the onset of a localized neck, or a shear localization.

The predicted fracture patterns are presented in Fig. 5 (b). All instances display fracture perpendicular to the transverse direction, approximately 50 mm away from the cup center. This is according to expectations, as the minimum strain ratio $R_\theta = d\varepsilon_w/d\varepsilon_t$ was observed at $\theta = 90^\circ$ (cf. Fig 2 (b)), indicating that the material is mostly prone to thinning when subjected to strains in this direction.

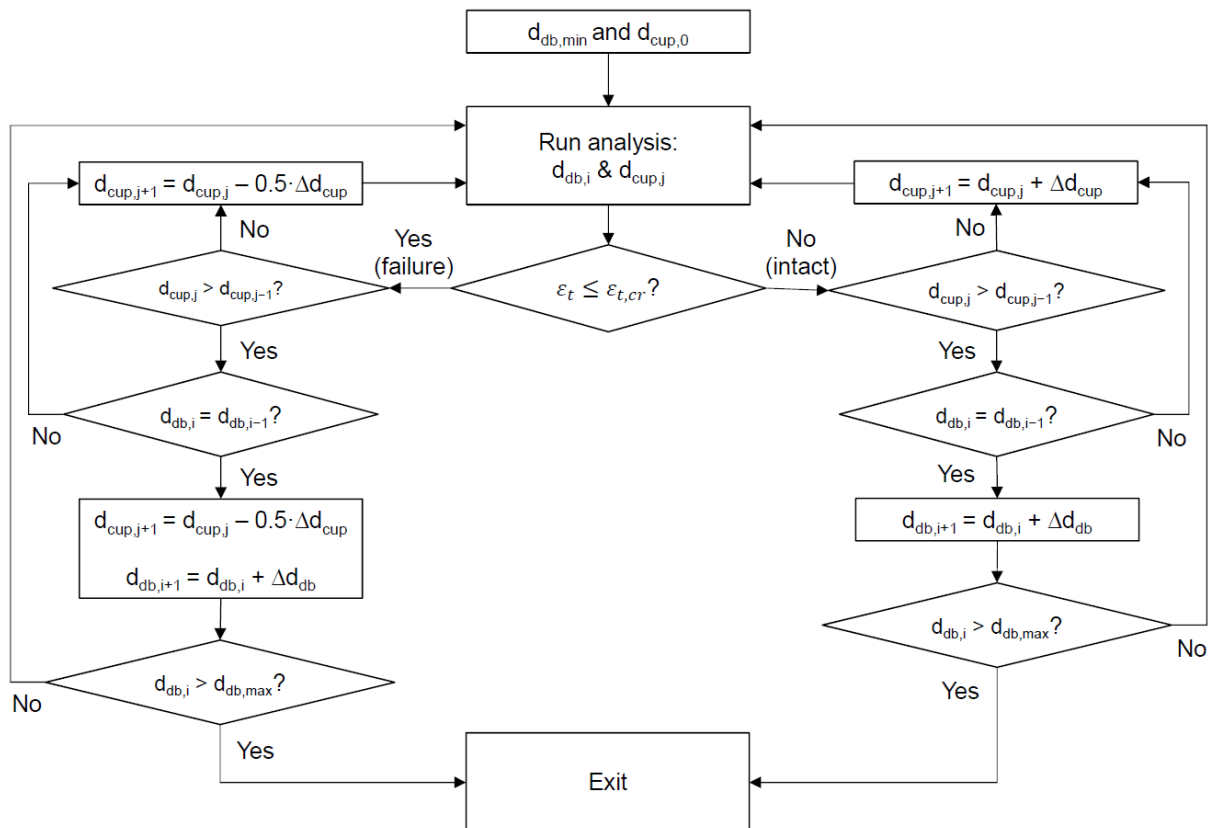


Fig. 4 Flowchart of algorithm for detection of the relationship between drawbead distance, and fracture cup depth.

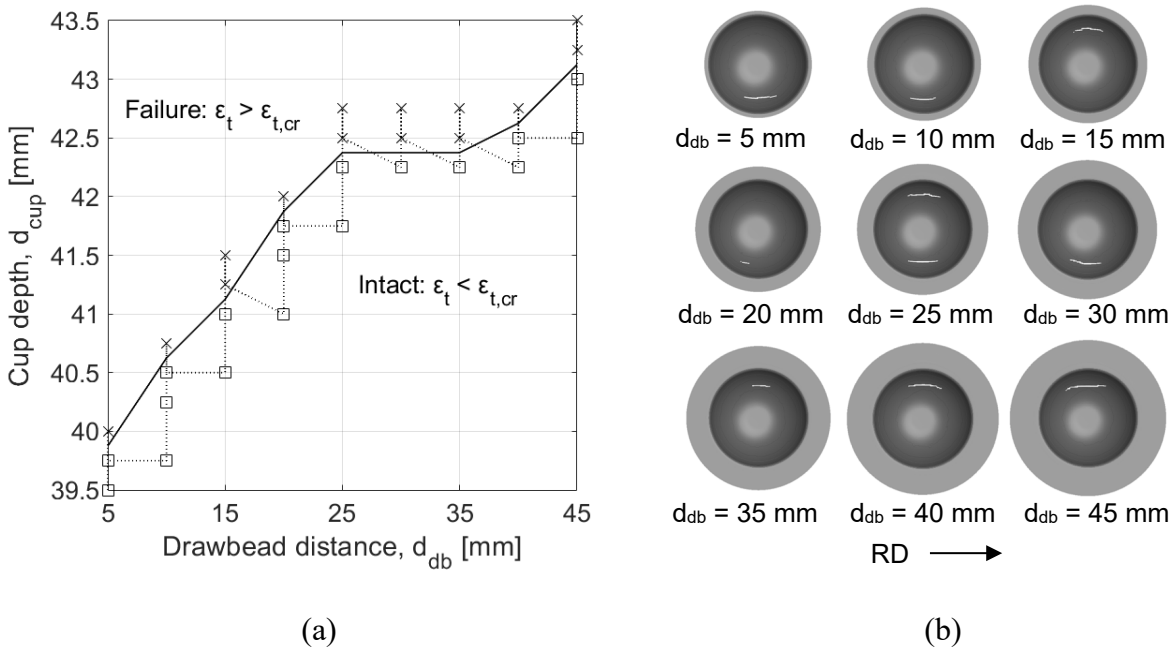


Fig. 5 (a) Fracture cup depth vs. drawbead distance. The error bars indicate the cup depth interval between the simulation that predicted failure, and the simulation that predicted an intact sheet. (b) Fracture patterns of the failed simulations.

Concluding remarks

In this preliminary study, the sheet metal forming process of a floating photovoltaic structure with a repeated cup feature was investigated through non-linear finite element analysis in LS-DYNA. The anisotropic Yld2003 yield criterion, and the isotropic two-term Voce hardening rule was calibrated to plasticity data from previous experimental tests of the 1.51 mm thick AA5083-H111 aluminum alloy sheets [17]. First, the cup geometry of the original design was assessed by varying the constant friction parameter, which proved to have a significant effect on the principal strain distribution and the critical cup depth. The results from these simulations were used along with the reported observations from preliminary experimental tests to estimate a constant friction parameter, and a critical thickness strain at fracture. Finally, the calibrated model was used in a parametric study, where a simple search algorithm was developed for the purpose of locating the failure limit in a two-dimensional parameter space.

The authors will continue with the work of developing a high-quality dataset for the training of a prediction model based on an artificial neural network. To this aim, the authors will focus on further developing the numerical simulation model, e.g. by implementing state-of-the-art criteria for the prediction of local necking, shear fracture, and ductile fracture, which governs the parametric forming limit. Since the case investigated in this study displayed a significant dependency on the constant friction parameter, a refined formulation that accounts for the static and dynamic contact friction would also be beneficial to ensure applicability to other geometric configurations. This calls for additional experimental tests to calibrate new model parameters, and to validate the FE model for various constellations of process parameters. Moreover, efforts will be dedicated to generalizing the simple search algorithm for extending its application to parameter spaces of higher dimensionality, starting with a review of existing approaches from the literature.

References

[1] LIVERMORE SOFTWARE TECHNOLOGY (LSTC), LS-DYNA® Theory Manual 2019.

- [2] A. Dal Pozzolo, O. Caelen, R.A. Johnson, G. Bontempi, Calibrating probability with undersampling for unbalanced classification, in: 2015 IEEE symposium series on computational intelligence, IEEE, 2015, pp. 159-166. <https://doi.org/10.1109/SSCI.2015.33>
- [3] D. Banabic, D.-S. Comsa, P. Eyckens, A. Kami, M. Gologanu, Advanced models for the prediction of forming limit curves, in: Multiscale Modelling in Sheet Metal Forming, 2016, pp. 205-300. https://doi.org/10.1007/978-3-319-44070-5_5
- [4] Z. Marciniak, K. Kuczyński, Limit strains in the processes of stretch-forming sheet metal, *Int. J. Mech. Sci.*, 9 (1967) 609-620. [https://doi.org/10.1016/0020-7403\(67\)90066-5](https://doi.org/10.1016/0020-7403(67)90066-5)
- [5] D. Banabic, A review on recent developments of Marciniak-Kuczynski model, *Comput. Methods in Mater. Sci.*, 10 (2010) 225-237
- [6] O. Lademo, T. Berstad, O. Hopperstad, K. Pedersen, A numerical tool for formability analysis of aluminium alloys. Part I: Theory, *Steel Grips*, 2 (2004) 427-431
- [7] O. Lademo, T. Berstad, O. Hopperstad, K. Pedersen, A numerical tool for formability analysis of aluminium alloys. Part II: Experimental validation, *Steel Grips*, 2 (2004) 433-437.
- [8] Ø. Fyllingen, O. Hopperstad, O.-G. Lademo, M. Langseth, Estimation of forming limit diagrams by the use of the finite element method and Monte Carlo simulation, *Comput. Struct.*, 87 (2009) 128-139. <https://doi.org/10.1016/j.compstruc.2008.07.002>
- [9] J.D. Bressan, J.A. Williams, The use of a shear instability criterion to predict local necking in sheet metal deformation, *Int. J. Mech. Sci.*, 25 (1983) 155-168. [https://doi.org/10.1016/0020-7403\(83\)90089-9](https://doi.org/10.1016/0020-7403(83)90089-9)
- [10] O. Hopperstad, T. Berstad, O. Lademo, M. Langseth, Shear instability criterion for plastic anisotropy, SINTEF, Trondheim, 2006.
- [11] A. Reyes, O.S. Hopperstad, T. Berstad, O.-G. Lademo, Prediction of necking for two aluminum alloys under non-proportional loading by using an FE-based approach, *Int. J. Mater. Form.*, 1 (2008) 211-232. <https://doi.org/10.1007/s12289-008-0384-6>
- [12] H. Aretz, A non-quadratic plane stress yield function for orthotropic sheet metals, *J. Mater. Process. Technol.*, 168 (2005) 1-9. <https://doi.org/10.1016/j.jmatprotec.2004.10.008>
- [13] E. Voce, The relationship between stress and strain for homogeneous deformation, *J. Inst. Met.*, 74 (1948) 537-562
- [14] Z. Marciniak, K. Kuczyński, T. Pokora, Influence of the plastic properties of a material on the forming limit diagram for sheet metal in tension, *Int. J. Mech. Sci.*, 15 (1973) 789-800. [https://doi.org/10.1016/0020-7403\(73\)90068-4](https://doi.org/10.1016/0020-7403(73)90068-4)
- [15] F. Barlat, J.C. Brem, J.W. Yoon, K. Chung, R.E. Dick, D.J. Lege, F. Pourghrat, S.H. Choi, E. Chu, Plane stress yield function for aluminum alloy sheets - part 1: theory, *Int. J. Plast.*, 19 (2003) 1297-1319. [https://doi.org/10.1016/S0749-6419\(02\)00019-0](https://doi.org/10.1016/S0749-6419(02)00019-0)
- [16] K.K. Phoon, S.P. Huang, S.T. Quek, Implementation of Karhunen–Loeve expansion for simulation using a wavelet-Galerkin scheme, *Probabilistic Eng. Mech.*, 17 (2002) 293-303. [https://doi.org/10.1016/S0266-8920\(02\)00013-9](https://doi.org/10.1016/S0266-8920(02)00013-9)
- [17] S. Tveit, A. Reyes, A submodeling technique for incorporating sheet metal forming effects in an AA5083 FPV structure, submitted for publication, (2024).